4. J. J. Mahoney, M. Storey, R. A. Duncan, K. J. Spencer, M. Pringle, in *The Mesozoic Pacific: Geology, Tectonics, and Volcanism*, M. Pringle, W. Sager, W. Sliter, S. Stein, Eds. (Monograph 77, American Geophysical Union, Washington, DC, 1993), pp. 233–261.
5. M. A. Richards, R. A. Duncan, V. E. Courtillot, *Science* **246**, 103 (1989); M. A. Richards, D. L. Jones, R. A. Duncan, D. J. DePaolo, *ibid.* **254**, 263 (1991); M. F. Coffin and O. Eldholm, *Geology* **21**, 515 (1993).
6. D. L. Anderson, *Geology* **22**, 39 (1994).
7. W. W. Sager *et al.*, *Initial Report of the Ocean Drilling Program* **143** (ODP, College Station, TX, 1993).
8. H. C. Jenkyns, *Proc. Ocean Drill. Prog. Sci. Results*, **143**, 99 (1995).
9. A. Arnaud-Vanneau and W. V. Sliter, *ibid.*, p. 537.
10. F. M. Gradstein *et al.*, *Geophys. Res.* **99**, 24051 (1994).
11. M. Pringle and R. Duncan, *Proc. Ocean Drill. Prog. Sci. Results* **143**, 277 (1995).
12. All samples were azimuthally unoriented. Samples were thermally demagnetized at a minimum of 16 steps to 650° to 680°C (shipboard alternating field demagnetizations were ineffective on some samples, indicating the presence of a high-coercivity phase). After the removal of one or more components at low (50° to 200°C) unblocking temperatures, most basalt samples displayed a simple univectorial decay.
13. D. V. Kent and J. Gee, *Science* **265**, 1561 (1994).
14. R. G. Gordon and A. Cox, *Geophys. J. R. Astron. Soc.* **63**, 619 (1980); A. Cox and R. G. Gordon, *Rev. Geophys.* **22**, 47 (1984).
15. P. L. McFadden and A. B. Reid, *Geophys. J. R. Astron. Soc.* **69**, 307 (1982).
16. M. Kono, *Init. Rep. Deep Sea Drill. Proj.* **55**, 737 (1980). Inclination groups are distinct (at the 95% confidence level) if $Z > 1.96$, where

$$Z = (\bar{I}_1 - \bar{I}_2)/\sqrt{\frac{\sigma_1^2}{n_1} - \frac{\sigma_2^2}{n_2}},$$

$\bar{I}_1$ and $\bar{I}_2$ are the means of two adjacent inclination groups, σ_1 and σ_2 are their standard deviations, and n_1 and n_2 are the number of samples used in each inclination group. Site 866 inclination units were divided as follows: A-B, B-C, and C-D by intervening boles; D-E by lithology; E-F by inclination; F-G and G-H by intervening boles; H-I by inclination; I-J by intervening bole; J-K by inclination; K-L by intervening bole; and L-M by magnetic polarity.
17. J. A. Tarduno, W. W. Sager, Y. Nogi, *Proc. Ocean Drill. Prog. Sci. Results* **143**, 395 (1995).
18. R. T. Merrill and M. W. McElhinny, *The Earth's Magnetic Field: Its History, Origin and Planetary Perspective* (Academic Press, San Diego, CA, 1983).
19. A. V. Cox, *Geophys. J. R. Astron. Soc.* **20**, 253 (1970).
20. P. L. McFadden, R. T. Merrill, M. W. McElhinny, S. Lee, *J. Geophys. Res.* **96**, 3923 (1991).
21. R. G. Gordon, *ibid.* **95**, 8397 (1990); W. W. Sager and M. S. Pringle, *ibid.* **93**, 11753 (1988); R. L. Larson and W. W. Sager, *Proc. Ocean Drill. Prog. Sci. Results* **129**, 471 (1992).
22. W. W. Sun and K. P. Kodama, *J. Geophys. Res.* **97**, 19599 (1992); P. Arason and S. Levi, *ibid.* **95**, 4501 (1990); R. L. Larson, M. B. Steiner, E. Erba, Y. Lancelot, *Proc. Ocean Drill. Prog. Sci. Results* **129**, 615 (1992).
23. W. W. Sager and J. A. Tarduno, *Proc. Ocean Drill. Prog. Sci. Results* **143**, 399 (1995).
24. J. A. Tarduno, *Geophys. Res. Lett.* **17**, 101 (1990). Because of their latitude dependence, compaction-induced errors can be detected by an internal comparison of sediment data representing a wide range of site latitudes. Through such comparisons, only three sites (sites 463, 865, and 866) may have yielded data unaffected by compaction. Sediments from site 463 may have escaped the effects of compaction because of early silicification. Results from sites 865 and 866 are derived from shallow water carbonate rocks, which preserve detailed sedimentary structures showing little compaction.
25. M. K. McNutt and A. V. Judge, *Science* **248**, 969 (1990); M. K. McNutt, E. L. Winterer, W. W. Sager, G. Ito, *Geophys. Res. Lett.* **17**, 1101 (1990).
26. E. L. Winterer and C. V. Metzler, *J. Geophys. Res.* **89**, 9969 (1984); R. A. Duncan and D. A. Clague, in *The Ocean Basin and Margins*, vol. 7, *The Pacific Ocean*, A. Nairn, F. G. Stehli, S. Uyeda, Eds. (Plenum, New York, 1985), pp. 89–121; E. L. Winterer *et al.*, in *The Mesozoic Pacific: Geology, Tectonics, and Volcanism*, M. Pringle, W. Sager, W. Sliter, S. Stein, Eds. (Monograph 77, American Geophysical Union, Washington, DC, 1993), pp. 307–334.
27. J. Phipps-Morgan and W. H. J. Smith, *Nature* **359**, 524 (1992).
28. J. E. T. Channell and E. Erba, *Earth Planet. Sci. Lett.* **108**, 161 (1992).
29. R. R. Castillo, P. A. Floyd, C. France-Lanord, *Proc. Ocean Drill. Prog. Sci. Results* **129**, 405 (1992).
30. W. H. F. Smith, H. Staudigel, A. B. Watts, M. S. Pringle, *J. Geophys. Res.* **94**, 10501 (1989).
31. W. Alvarez, D. V. Kent, I. Premoli Silva, R. A. Schweikert, R. A. Larson, *Geol. Soc. Am. Bull.* **91**, 476 (1980); J. A. Tarduno, M. McWilliams, N. Sleep, *J. Geophys. Res.* **95**, 15503 (1990); J. A. Tarduno and M. Myers, *ibid.* **99**, 21691 (1994).
32. D. C. Engebretson, A. Cox, R. G. Gordon, *Geol. Soc. Am. Spec. Pap.* **206** (1985).
33. H. Staudigel and S. D. King, *Earth Planet. Sci. Lett.* **109**, 517 (1992).
34. R. L. Larson and W. C. Pitman III, *Geol. Soc. Am. Bull.* **83**, 3645 (1972).
35. B. R. Globerman and E. Irving, *J. Geophys. Res.* **93**, 11721 (1988).
36. J. Besse and V. Courtillot, *ibid.* **96**, 4029 (1991).
37. G. M. Jones, *ibid.* **82**, 1703 (1977).

38. We thank the University of Rochester for support from the Rochester Paleomagnetic Laboratory and L. Tauxe for use of the SIO Paleomagnetics Laboratory. GMT software from P. Wessel and W. H. F. Smith was used to make figures in this paper, and software from R. Gordon was used to calculate the 129-Ma pole. Supported by NSF.

2 March 1995; accepted 23 May 1995

Protein Reaction Kinetics in a Room-Temperature Glass

Stephen J. Hagen, James Hofrichter, William A. Eaton

Protein reaction kinetics in aqueous solution at room temperature are often simplified by the thermal averaging of conformational substates. These substates exhibit widely varying reaction rates that are usually exposed by trapping in a glass at low temperature. Here, it is shown that the solvent viscosity, rather than the low temperature, is primarily responsible for the trapping. This was demonstrated by placement of myoglobin in a glass at room temperature and subsequent observation of inhomogeneous reaction kinetics. The high solvent viscosity slowed the rate of crossing the energy barriers that separated the substates and also suppressed any change in the average protein conformation after ligand dissociation.

A physical understanding of protein structure and function is becoming increasingly important to biology (*1*). Since the pioneering work of Austin and others (*2*), myoglobin (Mb) has been the paradigm for such studies. At temperatures below the glass transition of the solvent ($T_g \approx 180$ K for 3:1 glycerol-water mixtures), the geminate ligand rebinding kinetics of Mb after photodissociation of its carbon monoxide complex are widely distributed, extending from microseconds to kiloseconds. These kinetics have been explained by the simple idea that Mb molecules at low temperature are "frozen" into conformational substates, each binding with a different exponential rate (*2*). At room temperature in water, geminate rebinding is nearly exponential (*3*), which indicates that the energy barriers that separate substates are sufficiently low for thermal averaging to occur on the nanosecond time scale at which rebinding occurs. From a study of the viscosity dependence of the conformational relaxation after ligand dissociation in Mb, Ansari *et al.* (*4*) suggested that the trapping of conformational substates at low temperature may result more from high solvent viscosity than from energy barriers internal to the protein. Here, we confirm this hypothesis by showing that Mb embedded in a glass at room temperature exhibits ligand binding kinetics similar to those observed at low temperature. The ligand binding rates are distributed, and there is no evidence for conformational relaxation after ligand dissociation. The averaged geminate rebinding rates in the glass are much higher than those of the relaxed protein, which points to the functional consequence of conformational relaxation. These studies suggest a reinterpretation of previous low-temperature kinetic data as well as a clarification of the relation between kinetics, neutron-scattering experiments (*5*), and molecular dynamics simulations of "glass-like" transitions in proteins (*6*).

Conformational changes play an important role in the kinetics of Mb as well as of hemoglobin. In aqueous solution at room temperature, the geminate rebinding of carbon monoxide to Mb is much slower than predicted by an extrapolation of the low-temperature distribution of geminate rates (*3*). In addition, the average rate of geminate rebinding decreases as the temperature is increased through the solvent-glass transi-

Laboratory of Chemical Physics, Building 5, National Institutes of Health, Bethesda, MD 20892–0520, USA.

tion (2). This slowing of the kinetics was originally attributed to multiple geminate states that become accessible to the ligand at higher temperatures (2, 7). More recently, it has been explained by a structural relaxation of the protein that raises the average energy barrier for the ligand binding reaction but does not occur at low temperatures because it is frozen out (8, 9). This relaxation involves a displacement of globin atoms away from the heme and is caused by a displacement of the heme iron from the mean porphyrin plane upon ligand dissociation (10).

Spectroscopic observation of the structural relaxation (4, 11–14), as well as kinetic modeling (14), are consistent with this explanation. This relaxation in glycerol-water is highly extended in time, ranging from hundreds of femtoseconds to nearly 1 μs at 300 K (13), and its time course can be closely approximated by a stretched exponential function {that is, $\sim\exp[-(\kappa^* t)^{\beta}]$, where κ^* is the relaxation rate constant, t is time, and $\beta < 1$, determines the degree of the "stretch"}. Ansari *et al.* (4, 14) investigated the effect of solvent viscosity on the latter portion of this relaxation at solvent viscosities $\eta = 1$ to 300 centipoise (cP) and temperatures $T = 268$ to 308 K. They found that the relaxation rate exhibits a Kramers-like (15) inverse dependence on viscosity, such that

$$\kappa^* = [C/(\sigma + \eta)]\exp(-E_o/RT) \quad (1)$$

where $C \approx 7 \times 10^{10}$ cP/s, $R = 8.31$ J/mol K^{-1}, and $E_o \approx 10$ kJ/mol; $\sigma \approx 4$ cP represents the contribution of the protein to the total friction for the relaxation. Extrapolation of this result to the limit of a solvent glass transition, where η approaches 10^{15} cP (16), implies an overwhelming suppression of κ^* by the viscosity-dependent prefactor as T approaches T_g. The slowing of protein relaxation near T_g would then result not from energy barriers within the protein [the term $\exp(-E_o/RT)$ in Eq. 1], but from slow dynamics in crossing these barriers as a result of the friction imposed by the high solvent viscosity [the term $C/(\sigma + \eta)$ in Eq. 1]. Is this extrapolation valid? If so, is the rate of substate interconversion equally sensitive to viscosity? Ansari *et al.* (4) proposed that a sufficiently viscous solvent might suppress both interconversion and relaxation in Mb. Suppression of substate interconversion would give rise to inhomogeneous kinetics even at 300 K, whereas suppression of relaxation would yield faster rebinding (17).

To test this prediction, we studied ligand binding in the carbon monoxide complex of myoglobin (MbCO) embedded in a glass at room temperature. We prepared the sample by dehydrating a thin layer of a concentrated solution containing sperm whale MbCO, aqueous buffer, and a sugar, trehalose. The trehalose solution undergoes a glass transition upon drying (18), leaving MbCO embedded in a rigid ($\eta > 10^{15}$ cP) sugar matrix. The trehalose glass is presumed not to affect protein structure significantly, because trehalose occurs naturally at high concentration in the cells of many organisms that have adapted to survive extended periods of dehydration in arid environments (19). In fact, one mechanism proposed to explain anhydrobiosis is the formation of a trehalose glass in the cytoplasm upon dehydration, thereby arresting biochemical activity until water becomes available (18).

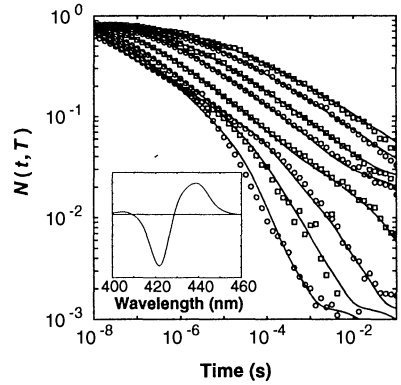

Fig. 1. The fraction $N(t,T)$ of molecules remaining unliganded at time t after photolysis. $N(t,T)$ was obtained from the amplitude of the average difference spectrum [basis spectrum ($U_1(\lambda)$ shown in inset]. The data (points) are for the temperatures (from bottom to top) 297, 254, 224, 187, 152, 135, 116, and 105 K. Time-resolved photolysis difference spectra of MbCO in trehalose were collected with a nanosecond spectrometer (30) and analyzed by singular value decomposition (SVD), which represents the data from all values of T and t in terms of a single set of basis spectra (31). The curves were obtained from a fit to the data with the use of the model of Eq. 2.

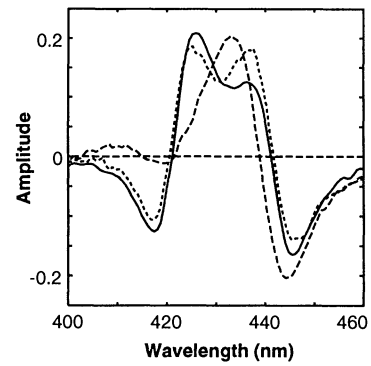

Fig. 2. Deviation from average difference spectrum [basis spectrum $U_2(\lambda)$] for Mb in room-temperature glass (solid line) and in a glycerol-water solution at 300 K (long dash) and at 190 K (short dash).

The population of unliganded protein molecules at times ranging from nanoseconds to milliseconds after photolysis of MbCO in trehalose was obtained from the overall amplitude of the photolysis difference spectrum (Fig. 1). Over the entire temperature range $T = 105$ to 297 K, the rebinding kinetics consist of a rapid and clearly nonexponential geminate process. The exponential and bimolecular rebinding present in fluid solvents near 300 K is not observed. Thus, we find near 300 K rebinding that resembles the low-temperature ($T < 200$ K) kinetics of MbCO in glycerol-water solvents. The simplest interpretation of this result is that the glassy solvent suppresses both interconversion of conformational substates and conformational relaxation at all temperatures. The following quantitative analysis of the data supports this conclusion.

The time-resolved photolysis difference spectra obtained for MbCO in the trehalose glass can be represented as linear combinations of two basis spectra (20, 21). The first spectrum, $U_1(\lambda)$ (where λ is the wavelength), is the average photolysis difference spectrum, and its time-dependent amplitude $V_1(t,T)$ accurately represents the ligand rebinding kinetics. The second spectrum, $U_2(\lambda)$, describes deviations from the average spectrum, and the time course of its amplitude $V_2(t,T)$ contains information about the protein conformation. The doubly peaked shape of $U_2(\lambda)$ (Fig. 2) approximates a derivative about the absorption maxima of Mb (≈432 nm) and MbCO (≈422 nm); $V_2(t,T)$ therefore describes a frequency shift of both the Mb and MbCO spectra toward shorter wavelengths during rebinding. A spectral shift of both peaks in the difference spectrum strongly indicates "kinetic hole burning," in which the spectra are inhomogeneously broadened and molecules that exhibit red-shifted Mb and MbCO spectra rebind at a faster than average rate (22). This spectral change is observed at all temperatures (with some differences that are a result of thermal broadening), which indicates that hole burning occurs even at 300 K. For comparison, Fig. 2 also shows $U_2(\lambda)$ observed for MbCO in a glycerol-water solution after nanosecond photolysis at $T = 190$ and 300 K. At 190 K, where rapid spectral changes arise from kinetic hole burning rather than from conformational relaxation (23), $U_2(\lambda)$ is similar to that observed at all temperatures in the trehalose sample. At 300 K, where the spectral changes in the glycerol-water solvent result from a relaxation of the Mb photoproduct (4, 11, 12, 14), $U_2(\lambda)$ in that solvent resembles a derivative of the Mb Soret peak alone, with little amplitude near the MbCO peak. Thus, qualitative analysis of the spectral changes described by $U_2(\lambda)$ indicates that they result from kinetic hole burning: even near 300 K, the glass suppresses both interconversion between conformational substates and protein relaxation for the duration of ligand rebinding.

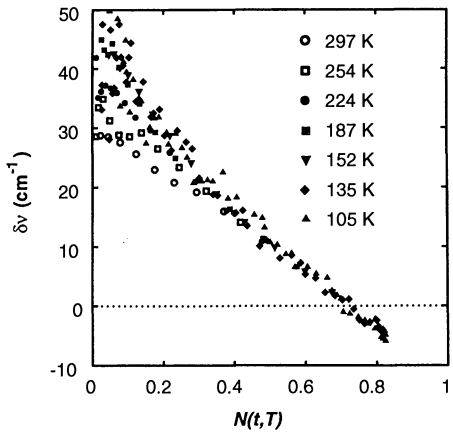

Fig. 3. Average spectral frequency shift $\delta\nu(t,T)$ of photolyzed molecules versus $N(t,T)$. Data from all values of T fall on essentially the same curve, which implies that spectral shifts during ligand recombination result from kinetic hole burning, rather than from conformational relaxation. The deviation for $T > 250$ K (at $N < 0.2$) can be attributed to population of the additional geminate state C.

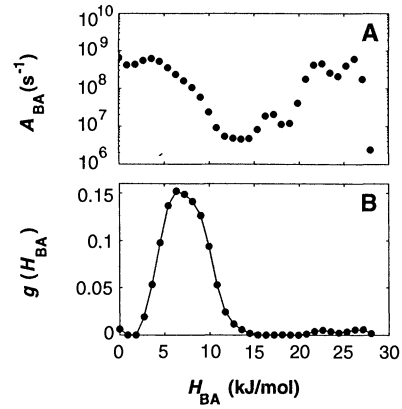

Fig. 4. (**A**) The rate prefactors $A_{BA}(H_{BA})$ and (**B**) the enthalpy distribution $g(H_{BA})$ obtained by fitting the ligand binding kinetics of Fig. 1 to the substate model for T = 105 to 297 K. We obtained a discrete approximation to $g(H_{BA})$ by considering m substates distributed uniformly over the interval H_{BA} = 0 to 28 kJ/mol. From H^i_{BA}, $A_{BA}(H^i_{BA})$, and the rates $k_{BC}(T)$ and $k_{CB}(T)$, the unliganded population N_i of each substate i from 1 to m is calculated as a function of t and T; $g(H^i_{BA})$ is then the weight with which substate i must contribute to the kinetics in order to fit the sum over the substates $\Sigma_i[g(H^i_{BA})N_i(t,T)]$ to the observed $N(t,T)$. The choice m = 32 minimizes the residuals.

Agmon and others (*23*, *24*) have discussed a "universal" behavior that provides a quantitative test for hole burning in inhomogeneous systems. If the absorption spectra of individual substates within the photolyzed population have a property $q = q(k)$ (where q = the center wavelength) that correlates with the substate rebinding rate k, a plot of the average $\langle q\rangle$ versus $N(t)$ measured during rebinding yields a curve that is nearly independent of temperature. This is true only if binding to each substate is a single exponential process, which is not the case if relaxation—that is, $q = q(k,t)$ and $k = k(q,t)$—occurs. In Fig. 3, the average spectral frequency shift $\delta\nu(t,T)$ [$\propto V_2(t,T)/V_1(t,T)$] of the unliganded molecules in the photolyzed sample is plotted against the unliganded population $N(t,T)$ [$\propto V_1(t,T)$] at several temperatures. This is analogous to a plot of $\langle q\rangle$ versus N. The data approximate a single curve for T = 105 to 297 K, which indicates that the spectral changes result from hole burning rather than from protein relaxation. Deviations become significant only above 250 K for values of N less than about 0.2, where an additional ligand state complicates rebinding and the above test cannot apply (*21*).

Motivated by the observation of a distribution of ligand rebinding rates (Fig. 1) and by the spectral evidence for kinetic hole burning (Figs. 2 and 3), we have fitted $N(t,T)$ to an inhomogeneous, nonrelaxing substate model (*2*, *7*):

$$\begin{aligned} A_1 &\leftarrow B_1 \leftrightarrows C_1 \\ A_2 &\leftarrow B_2 \leftrightarrows C_2 \\ &\vdots \\ A_m &\leftarrow B_m \leftrightarrows C_m \end{aligned} \qquad (2)$$

We assume that a CO molecule can move between three sites within the protein: A, B, and C. Photolysis dissociates the ligand from the bound state A to an unbound state B with the CO adjacent to the heme, from which it rebinds by thermal activation over a barrier of height H_{BA}. The rate of passage from B to A is $k_{BA} = A_{BA}(T/T_o)\exp(-H_{BA}/RT)$, where T_o = 180 K and the prefactor A_{BA} has the dimension 1/seconds. The second geminate state C corresponds to the ligand located at an additional site in the protein more distant from the heme and accessible from B. The rate of passage between B and C is determined by energy barriers H_{BC} and H_{CB} and rate prefactors A_{BC}, A_{CB}. Each of the m structural substates of the protein is assumed to have a different value for H_{BA}: a function $g(H_{BA})$ gives the fraction of molecules occupying the substate characterized by a given value of H_{BA}. Unlike previous authors, we allow the rate prefactor A_{BA} to vary among substates (*25*). A fit to $N(t,T)$ yields $g(H_{BA})$ and the other parameters of the model.

The inhomogeneous model provides good agreement with the data over the entire temperature range (Fig. 1), which indicates that substate interconversion is suppressed even near 300 K. The resulting $g(H_{BA})$ (Fig. 4B) is a smooth, nearly symmetric distribution peaked at $H_{BA} \approx 6.3$ kJ/mol, with a full-width at half-maximum of 6.3 kJ/mol. Unlike A_{BA} in glycerol-water solvents, which is relatively independent of H_{BA}, A_{BA} in trehalose falls almost exponentially as H_{BA} increases ($A_{BA}^{max}/A_{BA}^{min} \sim 10^2$) (Fig. 4A). State C contributes little to the kinetics except near room temperature, because $H_{BC} \approx 38$ kJ/mol and $H_{CB} \approx 34$ kJ/mol are large values.

Because the kinetic and spectral evidence show that neither substate interconversion nor conformational relaxation occurs from 10 ns to 100 ms after photolysis in the glassy solvent, we conclude that the resulting $g(H_{BA})$ represents the enthalpy distribution of the unrelaxed protein. The substate-averaged CO rebinding rate for unrelaxed Mb at 300 K is then calculated to be $\langle k_{BA}\rangle \approx 5.1 \times 10^7\ s^{-1}$, ~2500 times greater than the rate $\langle k_{BA}\rangle \approx 2 \times 10^4\ s^{-1}$ observed for the fully relaxed protein in aqueous solvents (*14*). This confirms the hypothesis that relaxation of Mb raises the average barrier $\langle H_{BA}\rangle$ and therefore slows ligand rebinding (*8*, *9*, *14*).

Because of the Kramers-like relaxation rate shown in Eq. 1, it is likely that exponential growth of solvent viscosity near the solvent glass transition, rather than high energy barriers, accounts for the slow Mb conformational dynamics observed in previous low-temperature studies. Those studies may therefore have revealed more about the low-temperature viscosity of glycerol-water mixtures than about the energy barriers separating protein conformational substates (*26*). The fact that functionally significant conformational changes are sensitive to viscosity suggests that they correspond to small motions of the protein molecule that displace the solvent, such as a slight repositioning of the helices. This is in contrast to isolated local motions such as side chain rotations, which exhibit a "glass-like" transition near 200 K in neutron-scattering (*5*) and molecular dynamics (*6*) studies of slightly hydrated Mb. Recent experiments on conformational equilibration in slightly hydrated Mb support this view (and also may allow a determination of the size of the energy barriers separating protein conformations). In the absence of a glassy solvent, conformational transitions are observed at temperatures at least as low as 78 K (*27*). Evidently, a glass transition is not necessarily a feature of the conformational kinetics of the protein (*28*).

Recent x-ray studies have suggested that conformational relaxation can occur in a protein embedded in a solid at low temperatures (*29*); the viscosity dependence of this relaxation must differ from that shown in Eq. 1 to allow a finite rate in the limit of infinite solvent viscosity. Our kinetic data suggest that this relaxation either (i) occurs outside our experimental time window at temperatures between 100 and 300 K or (ii) is spectroscopically invisible and does not influence the ligand rebinding kinetics.

Finally, it is interesting to note that, in fluid solvents, the earliest spectroscopic changes observed in Mb at room temperature occur within a few picoseconds of photodissociation (*13*). Because this time scale is comparable to the shear relaxation time of the aqueous solvent, the solvent response to the fastest conformational changes is expected to resemble that of an elastic solid. Picosecond-resolved optical studies of our system may therefore show that the fastest conformational changes of a protein appear similar in water and in a glass.

REFERENCES AND NOTES

1. H. Frauenfelder and P. G. Wolynes, *Science* **229**, 337 (1985); H. Frauenfelder, S. G. Sligar, P. G. Wolynes, *ibid.* **254**, 1598 (1991); H. Frauenfelder and P. Wolynes, *Phys. Today* **47**, 58 (1994).
2. R. H. Austin, K. W. Beeson, L. Eisenstein, H. Frauenfelder, I. C. Gunsalus, *Biochemistry* **14**, 5355 (1975).
3. E. R. Henry, J. H. Sommer, J. Hofrichter, W. A. Eaton, *J. Mol. Biol.* **166**, 443 (1983).
4. A. Ansari, C. M. Jones, E. R. Henry, J. Hofrichter, W. A. Eaton, *Science* **256**, 1796 (1992).
5. W. Doster, S. Cusack, W. Petry, *Nature* **337**, 754 (1989).
6. R. J. Loncharich and B. R. Brooks, *J. Mol. Biol.* **215**, 439 (1990); J. Smith, K. Kuczera, M. Karplus *Proc. Natl. Acad. Sci. U.S.A.* **87**, 1601 (1990).
7. D. Beece *et al.*, *Biochemistry* **19**, 5147 (1980).
8. N. Agmon and J. Hopfield, *J. Chem. Phys.* **79**, 2042 (1983); E. R. Henry, J. Hofrichter, J. H. Sommer, W. A. Eaton, in *Hemoglobins: Structure and Function*, A. Schnek and C. Paul, Eds. (Edition de l'Université de Bruxelles, Brussels, 1983), pp. 193–203; J. Hofrichter *et al.*, *Biochemistry* **24**, 2667 (1985).
9. P. J. Steinbach *et al.*, *Biochemistry* **30**, 3988 (1991).
10. J. Kuriyan, S. Wilz, M. Karplus, G. Petsko, *J. Mol. Biol.* **192**, 133 (1986).
11. D. G. Lambright, S. Balasubramanian, S. G. Boxer, *Chem. Phys.* **158**, 249 (1991).
12. W. D. Tian, J. T. Sage, V. Šrajer, P. M. Champion, *Phys. Rev. Lett.* **68**, 408 (1992).
13. M. Lim, T. A. Jackson, P. A. Anfinrud, *Proc. Natl. Acad. Sci. U.S.A.* **90**, 5801 (1993); T. A. Jackson, M. Lim, P. A. Anfinrud, *Chem. Phys.* **180**, 131 (1994).
14. A. Ansari, C. M. Jones, E. R. Henry, J. Hofrichter, W. A. Eaton, *Biochemistry* **33**, 5128 (1994).
15. H. A. Kramers, *Physica* **7**, 284 (1940); P. Hänggi, P. Talkner, M. Borkovec, *Rev. Modern Phys.* **62**, 251 (1990).
16. J. Jäckle, *Rep. Progr. Phys.* **49**, 171 (1986); C. A. Angell, *Science* **267**, 1924 (1995).
17. A model clarifying the relation between interconversion of conformational substates and the stretched exponential time course of conformational relaxation has been proposed by S. J. Hagen and W. A. Eaton (unpublished results). In this model the stretched relaxation reflects a redistribution of molecules from one distribution of conformational substates to another at lower energy, subject to the simple kinetic rule that all transition states are at approximately the same energy. The stretched exponential is a natural consequence of the interconversion of substates occurring on the same time scale as the change in the overall average structure of the molecule. Interconversion of conformational substates and conformational relaxation are parts of the same process.
18. J. L. Green and C. A. Angell, *J. Phys. Chem.* **93**, 2880 (1989).
19. C. Womersley, *Comp. Biochem. Physiol.* **70B**, 669 (1981); J. H. Crowe, L. M. Crowe, J. F. Carpenter, C. Aurell Wistrom, *Biochem. J.* **242**, 1 (1987).
20. Before analysis of the data, it was essential to correct the raw photolysis difference spectra for the intrinsic temperature dependence of both the Mb and MbCO spectra. This multistep correction is described elsewhere (*21*).
21. S. J. Hagen, J. Hofrichter, W. A. Eaton, unpublished results.
22. B. F. Campbell, M. R. Chance, J. M. Friedman, *Science* **238**, 373 (1987).
23. V. Šrajer and P. Champion, *Biochemistry* **30**, 7390 (1991).
24. N. Agmon, *ibid.* **27**, 3507 (1988); N. Agmon, *J. Phys. Chem.* **94**, 2959 (1990).
25. Because this model treats the protein and its environment as stiff and nonrelaxing on the time scale of ligand rebinding, the solvent does not exert dissipative influences that affect the diffusion constant of the moving ligand; we therefore do not include a solvent-viscosity dependence in these rates [N. Agmon and S. Rabinovich, *J. Chem. Phys.* **97**, 7270 (1992)].
26. Previous studies on Mb embedded in polyvinyl alcohol (PVA) discussed the question of the suppression of conformational substate interconversion in solid media (*2*) [A. Ansari *et al.*, *Biophys. Chem.* **26**, 337 (1987); I. Iben *et al.*, *Phys. Rev. Lett.* **62**, 1916 (1989)]. However, Mb in PVA shows complex and multiphasic kinetics above 200 K. These cannot be interpreted in the absence of spectral data on kinetic hole burning and conformational relaxation. Furthermore, the crossing of the ligand rebinding curves at different temperatures in PVA implies conformational relaxation as the explanation for the multiple nonexponential phases (*9*).
27. E. Mayer, *Biophys. J.* **67**, 862 (1994); W. Doster, T. Kleinert, F. Post, M. Settles, in *Protein-Solvent Interactions*, R. Gregory, Ed. (Dekker, New York, 1993), pp 375–385.
28. J. L. Green, J. Fan, C. A. Angell, *J. Phys. Chem.* **98**, 13780 (1994).
29. I. Schlichting, J. Berendzen, G. N. Phillips, R. M. Sweet, *Nature* **371**, 808 (1994); T.-Y. Teng, V. Šrajer, K. Moffat, *Nature Struct. Biol.* **1**, 701 (1994).
30. J. Hofrichter *et al.*, *Methods Enzymol.* **232**, 387 (1994).
31. E. R. Henry and J. Hofrichter, *ibid.* **210**, 129 (1992).

32. We thank A. Szabo, P. Wolynes, and R. Zwanzig for helpful discussions and C. Austen Angell for suggesting the use of trehalose as a glass.

29 March 1995; accepted 12 June 1995

Binding of CO to Myoglobin from a Heme Pocket Docking Site to Form Nearly Linear Fe–C–O

Manho Lim, Timothy A. Jackson, Philip A. Anfinrud*

The relative orientations of carbon monoxide (CO) bound to and photodissociated from myoglobin in solution have been determined with time-resolved infrared polarization spectroscopy. The bound CO is oriented ≤7 degrees from the heme normal, corresponding to nearly linear Fe–C–O. Upon dissociation from the Fe, CO becomes trapped in a docking site that orientationally constrains it to lie approximately in the plane of the heme. Because the bound and "docked" CO are oriented in nearly orthogonal directions, CO binding from the docking site is suppressed. These solution results help to establish how myoglobin discriminates against CO, a controversial issue dominated by the misconception that Fe–C–O is bent.

To understand how the structure of a protein affects its function, it is crucial to know the structures of intermediates in the reaction pathway. Myoglobin (Mb), a protein that reversibly binds small ligands such as O_2 and CO, has long served as a model system for probing protein control of ligand binding and discrimination (*1*). The active binding site in Mb consists of an iron(II)-containing porphyrin, known as a heme, embedded within the hydrophobic interior of the globular protein. It is well known that the protein environment modulates the activity and selectivity of the heme: CO binds to free heme about 10^3 to 10^4 times as strongly as O_2 (*2*) but binds to the heme in Mb only 30 times as strongly as O_2 (*3*). Because CO is produced endogenously by the metabolism of heme (*4*), discrimination against this toxic ligand is thought to be biologically important.

A structural basis for discrimination against CO was implicated by the crystal structures of liganded Mb and model heme compounds: it was found that CO binds to Mb in a bent Fe–C–O geometry (*5*) but binds to model hemes in a linear geometry (*6*). It was presumed that the protein forces CO to bind in a bent geometry, thereby reducing the affinity of the heme for CO (*2*, *7*). Because O_2 binds to Mb (*8*) and model hemes (*9*) in a similar bent configuration, the steric hindrance imposed by the protein on bound O_2 was presumed to be negligible. This mechanism for reducing the binding affinity of Mb for CO seems compelling. Indeed, it has become a classic example of the relation between structure and function in proteins (*10*). However, the premise that Fe–C–O is bent in MbCO (*11*, *12*) and the assumption that bending is functionally important (*13*) remain controversial.

The angle of CO relative to the heme plane normal of MbCO has been determined by a variety of techniques, some of which are detailed in Table 1. The x-ray and neutron diffraction crystal structures provide the strongest evidence for a bent Fe–C–O, with the CO orientation ranging from 19° to 60°. The discrepancies between $P2_1$ and *P*6 crystal structures might result from differences in crystal packing: *P*6 crystals contain more water and therefore might be a better model for MbCO in solution

Department of Chemistry, Harvard University, Cambridge, MA 02138, USA.

*To whom correspondence should be addressed.